Article

Not peer-reviewed version

Ramsey Approach to Hamiltonian Mechanics

Edward Bormashenko * , Shraga Shoval , Ramita Sarkar

Posted Date: 5 December 2025

doi: 10.20944/preprints202512.0575.v1

Keywords: Hamiltonian mechanics; Poisson brackets; graph theory; bi-colored graph; Ramsey numbers; Shannon entropy

Preprints.org (www.preprints.org) | NOT PEER-REVIEWED | Posted: 5 December 2025 doi:10.20944/preprints202512.0575.v1

Article

Ramsey Approach to Hamiltonian Mechanics

Edward Bormashenko [1,*], Shraga Shoval [2] and Ramita Sarkar [1,2]

[1] Department of Chemical Engineering, Ariel University, Ariel, POB 3, 407000, Israel

[2] Department of Industrial Engineering and Management, Faculty of Engineering, Ariel University, P.O. Box 3, Ariel 407000, Israel

* Correspondence: edward@ariel.ac.il

Abstract

We introduce a new combinatorial framework for classical mechanics - the Ramsey -Hamiltonian approach - which interprets Poisson-bracket relations through the lens of finite and infinite Ramsey theory. Classical Hamiltonian mechanics is built upon the algebraic structure of Poisson brackets, which encode dynamical couplings, symmetries, and conservation laws. We reinterpret this structure as a bi-colored complete graph, whose vertices represent phase-space observables and whose edges are colored gold or silver according to whether the corresponding Poisson bracket vanishes or not. Because Poisson brackets are invariant under canonical transformations (including their centrally extended Galilean form), the induced graph coloring is itself a canonical invariant. Applying Ramsey theory to this graph yields a universal structural result: any six observables necessarily form at least one monochromatic triangle, independent of the Hamiltonian's specific form. Gold triangles correspond to mutually commuting (Liouville-compatible) observables that generate Abelian symmetry subalgebras, whereas silver triangles correspond to fully interacting triplets of dynamical quantities. When the Hamiltonian is included as a vertex, the resulting Hamilton–Poisson graphs provide a direct graphical interpretation of Noether symmetries, cyclic coordinates, and conserved quantities through star-like subgraphs centered on the Hamiltonian. We further extend the framework to Hamiltonian systems with countably infinite degrees of freedom - such as vibrating strings or field-theoretic systems - where the infinite Ramsey theorem guarantees the existence of infinite monochromatic cliques of observables. Finally, we introduce Shannon-type entropy measures to quantify structural order in Hamilton–Poisson graphs through the distribution of monochromatic polygons. The Ramsey–Hamiltonian approach offers a novel, symmetry-preserving, and fully combinatorial reinterpretation of classical mechanics, revealing universal dynamical patterns that must occur in every Hamiltonian system regardless of its detailed structure.

Keywords: Hamiltonian mechanics; Poisson brackets; graph theory; bi-colored graph; Ramsey numbers; Shannon entropy

---

1. Introduction

In the present paper we introduce the Ramsey interpretation of the classical Hamiltonian mechanics. Classical Hamiltonian mechanics provides a general, powerful and elegant way to describe the dynamics of a system [1–4]. It is particularly fruitful in physics, engineering, and mathematical physics because it offers deep and fruitful insights into conservation laws, symmetries, and the connection between classical and quantum mechanics [1–4]. The Poisson bracket structure of classical mechanics translates into the quantum commutator according to Eq. 1:

$$\{A,B\} \to \frac{1}{i\hbar}\left[\hat{A},\hat{B}\right]. \tag{1}$$

Hamiltonian mechanics emphasizes and effectively exploits symmetry properties, leveraging seminal Noether's theorem to connect symmetries with conserved quantities like linear and angular momentum [1–4]. Generalized Hamiltonian formalism for field theory was developed [5]. The

 doi:10.20944/preprints202512.0575.v1

geometric formulation of autonomous Hamiltonian mechanics in the terms of symplectic and Poisson manifolds was developed [6,7].

We develop the alternative Ramsey-Hamilton approach to the classical mechanics. Ramsey theory is a branch of mathematics/combinatorics/graph theory that studies conditions under which "order" must appear in large and complex structures [8–14]. It reveals unavoidable patterns in sufficiently large mathematical objects, even when those objects are chosen arbitrarily [8–14]. The fundamental idea is that in a large enough system, some form of structure/pattern or regularity is inevitable, no matter how the system is arranged. This is often expressed through the phrase: "Complete disorder is impossible" [8–14]. Consider a famous "party problem". We address a group of six people at a party. If each pair of people is either friends or strangers, then among these six people, there will always be a group of three who are mutual "friends" or a group of three persons who are mutual "strangers". Thus, the Ramsey number emerges, $R(3,3) = 6$.

Ramsey's theorem re-formulated in the language of the graphs theory, states that for any given number of colors and any given size of a graph, there exists a sufficiently large structure where some sub-graph must be necessarily monochromatic (i.e., all elements of that subset are the same color). Thus, in the complete bi-colored graph containing six vertices, at least one mono-colored triangle will necessarily appear. The Ramsey theory considers objects, seen as the vertices of the graphs and relations between these objects, seen as the links/edges of the graph. Thus, it supplies the very general framework for the treatment of physical problems. At the same time, the applications of the Ramsey theory to physics are still scarce [15–21]. We introduce the Ramsey framework for the classical physics, exploiting the properties of the Poisson brackets. The introduced Ramsey–Hamiltonian approach encodes Poisson relationships into a finite bi-colored graph and then applies combinatorial (Ramsey-type) theorems to deduce structural constraints that must exist in any finite configuration of functions. This is a novel, cross-disciplinary viewpoint: using unconditional combinatorial existence theorems (e.g., guaranteed monochromatic subgraphs) to deduce necessarily-occurring dynamical relations. The Ramsey re-interpretation of the Hamiltonian mechanics enables a new look on the symmetries of mechanical systems. We also address the infinite Ramsey theory based interpretation of the classical mechanics.

2. Hamiltonian Mechanics: Ramsey Interpretation

2.1. Bi-Colored Complete Graph Corresponding to the Hamiltonian Systems

Consider the system described by the Hamiltonian $H(p_i, q_i, i = 1, \dots, N)$. For a sake of simplicity we address the system, in which Hamiltonian does not explicitly depend on time. Consider set of the functions/observables: $f_1(p_i, q_i), \dots. f_6(p_i, q_i)$. The Poisson brackets are defined with Eq. (2):

$$\{f_l, f_m\} = \sum_{i=1}^{N} \left(\frac{\partial f_l}{\partial q_i}\frac{\partial f_m}{\partial p_i} - \frac{\partial f_l}{\partial p_i}\frac{\partial f_m}{\partial q_i}\right). \quad (2)$$

Consider now bi-colored, complete Ramsey graph. Functions: $f_1(p_i, q_i), \dots. f_6(p_i, q_i)$ serve as the vertices of the graph. Vertices of the graph are connected with the gold link, when Eq. 3 takes place (see **Figure 1A**):

$$\{f_l, f_m\} = 0. \quad (3)$$

Vertices of the graph are connected, in turn, with the silver link, when Eq. 4 takes place (see **Figure 1B**):

$$\{f_l, f_m\} = -\{f_m, f_l\} \neq 0. \quad (4)$$

Figure 1. Coloring of the graph is depicted. The vertices are functions defined in the phase space of the physical system. **A**. Vertices are connected with the gold link; $\{f_1, f_2\} = 0$ takes place. **B**. Vertices are connected with the silver link, when $\{f_3, f_4\} \neq 0$ is true.

It should be emphasized, that the aforementioned coloring, introduced with Eqs. 3-4, remains the same under the canonical transformations: $(q_i, p_i) \rightarrow (Q_i(q_i, p_i), P_i(q_i, p_i))$, due to the fact that canonical transformations remain the Poisson brackets the same, namely: $\{f, g\}_{q,p} = \{f, g\}_{Q,P}$. Thus, the introduced coloring remains untouched under linear symplectic transformation (rotations in phase space) and point transformations. And, it is important that the introduced coloring remains the same under centrally extended Galilean transformations (Bargmann group), which are the subset of the canonical transformations (we restrict ourselves with the classical mechanics). This conclusion stems from the fact that the Poisson brackets are invariant relatively to Galilean transformations up to a central extension, which is necessary to describe systems with nonzero mass, which implies $\{C_i, p_j\} = m\delta_{ij}$, where C_i is the generator of rotationless Galilean transformations (Galileian boosts), and m is the mass. Coloring defined by Eq.3-4 remains the same for centrally extended Galilean transformations.

2.2. Properties of the Poisson Graphs

Now we address the hypothetic graph emerging from the set of the aforementioned functions: $f_1(p_i, q_i), \ldots . f_6(p_i, q_i)$ depicted in **Figure 2**. We consider this graph below as the Poisson graph.

The Ramsey theory states that the graph, depicted in **Figure 2** inevitably contains at least one mono-colored triangle. Indeed, triangle (f_1, f_4, f_6) is a monochromatic gold; whereas the triangle (f_1, f_3, f_5) is a monochromatic silver one. Consider the gold triangle (f_1, f_4, f_6) and address the general properties of gold triangles. Within the gold triangles $\{f_l, f_m\} = 0$. This means that functions constituting gold triangle are Liouville compatible. In other words, three functions f_1, f_4 and f_6 are mutually conserved under Hamiltonian evolution, since the Poisson bracket measures how one function changes along the flow generated by the other. Thus, three functions f_1, f_4 and f_6 are symmetries each to other. These functions generate an Abelian subalgebra of phase–space symmetries and can be simultaneously used as coordinates on invariant surfaces of motion.

Preprints.org (www.preprints.org) | NOT PEER-REVIEWED | Posted: 5 December 2025 doi:10.20944/preprints202512.0575.v1

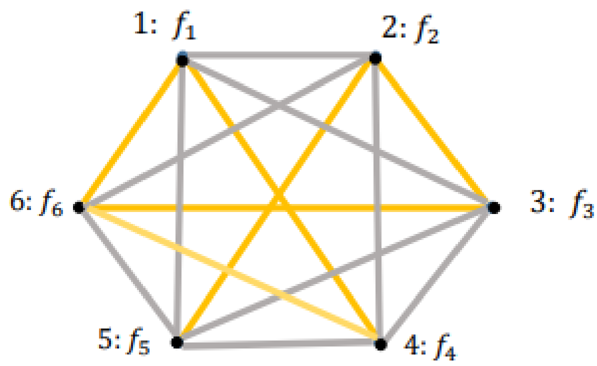

Figure 2. Colored graph defined by Eqs. (3-4) is depicted. Functions: $f_1(p_i,q_i),\dots,f_6(p_i,q_i)$/ Vertices of the graph are connected with the gold link, when $\{f_l,f_m\}=0$ takes place. Vertices of the graph are connected with the silver link, when $\{f_l,f_m\}\neq 0$ is true.

The complete, bi-colored graph shown in **Figure 2** necessarily consists at least one mono-chromatic triangle, due to the fact that the Ramsey number $R(3{,}3)=6$. Thus, the following theorem emerges:

Theorem 1. Consider the system described by the Hamiltonian $H(p_i,q_i,i=1,\dots,N)$. Hamiltonian does not explicitly depend on time. Consider set of the functions/obervables: $f_1(p_i,q_i),\dots.f_6(p_i,q_i)$ serving the vertices of the graph. Vertices of the graph are connected with the gold link, when $\{f_l,f_m\}=0$ takes place; they are connected with the silver link, when $\{f_l,f_m\}\neq 0$ is true. The emerging complete bi-colored graph contains at least one monochromatic triangle. The coloring of the graph remains the same under the canonical transformations

It should be emphasized, that **Theorem 1** is based on pure combinatorics considerations, and it is true for any Hamiltonian system. It is completely disconnected from the shape of the specific Hamiltonian. Now we address the properties of monochromatic silver triangles, such as the triangle (f_1,f_3,f_5) in **Figure 2**. No two functions constituting the vertices of these triangles can be simultaneously conserved or mutually diagonalized. Thus, a silver triangle signals a cluster of mutually coupled dynamical quantities. Regrettably, the Ramsey theory does not predict the exact color of the mono-colored triangle to be necessarily present in the graph [9–13].

It is noteworthy that permutations of the functions $f_1(p_i,q_i),\dots.f_6(p_i,q_i)$ do not influence the presence of the monochromatic triangles in the graph. This follows from simple combinatorics considerations. It is also important that the coloring of the graph defined by Eqs. (3-4) is non-transitive. This means that if $\{f_l,f_m\}=0$ and $\{f_m,f_k\}=0$ takes place, it does not necessarily imply $\{f_l,f_k\}=0$. This is crucial for our analysis, due to the fact that the relations of transitivity change the values of Ramsey numbers for the bi-colored, complete graphs [22]. And it should be emphasized that if f_1 and f_2 are the integrals of motion (i.e. $\{H,f_1\}=0$) and $\{H,f_2\}=0$ is true, it means that $\{f_1,f_2\}=const.$ This constant does not necessarily equal zero. Thus, the suggested coloring procedure is not necessarily transitive when f_1 and f_2 are the integrals of motion.

Now consider the hypothetic graph, depicted in **Figure 3**. Now, one of the functions is the Hamiltonian of the system itself, i.e. $f_1=H(p_i,q_i,i=1,\dots,N)$.

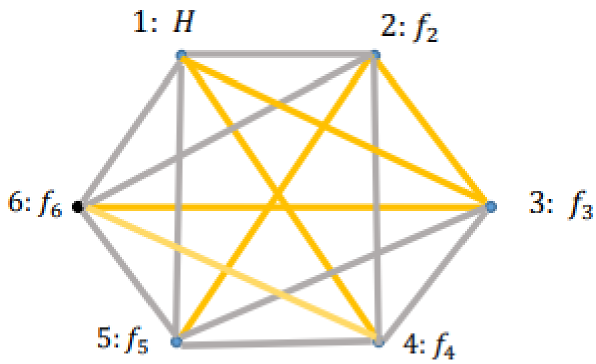

Figure 3. Bi-colored hypothetic graph generated by the functions $H(p_i, q_i), f_2(p_i, q_i), \ldots, f_5(p_i, q_i)$ is depicted. The coloring of the links corresponds to that depicted in **Figure 2**.

We consider below this graph, as the "Hamilton-Poisson graph". Again, it is assumed that the Hamiltonian does not explicitly depend on time. We recognize from the graph, depicted in Figure that $\{H, f_3\} = 0$ and $\{H, f_4\} = 0$. This does not imply that $\{f_3, f_4\} = 0$. From the Jacobi identity:

$$\{H\{f_3, f_4\}\} = \{\{H, f_3\}, f_4\} + \{f_3[H, f_4]\} = 0, \tag{5}$$

if $\{H, f_3\} = 0$ and $\{H, f_4\} = 0$ then the right-hand side vanishes, so we calculate:

$$\{H\{f_3, f_4\}\} = 0. \tag{6}$$

Thus, $\{f_3, f_4\}$ is a conserved quantity (due to the fact that Poisson brackets commute with H). But conservation does not necessarily imply that the bracket itself is zero. In other words, $\{f_3, f_4\}$ is constant along the Hamiltonian flow, but that constant may be nonzero. We conclude, that introduced coloring is non-transitive. There is no monochromatic gold triangle in **Figure 3**. If such a triangle, containing H is present in the graph, his vertices (together with the Hamiltonian) form a compatible triple in Liouville sense. However, at least one monochromatic triangle should necessarily be present in the graph. Triangles $\{H, f_5, f_6\}$ and $\{f_3, f_4, f_5\}$ are monochromatic silver. This means that neither f_5 nor f_6 is conserved under the evolution generated by H, i.e. H, f_5 and f_6 form a fully interacting triple. No two functions from the triple $\{f_3, f_4, f_5\}$ can be simultaneously conserved or mutually diagonalized. It is also noteworthy, that canonical transformations $Q_i = p_i, P_i = -q_i$ remain coloring of the Ramsey-Hamilton graph unchanged [1].

Examples of the Hamilton-Poisson graphs constructed for the harmonic oscillator and the two-body problem are supplied in **Appendix 1**. The Hamilton-Poisson graph emerging for the rotation of a rigid body is presented in **Appendix 2**. Analysis of the Hamilton-Poisson graph obtained for the two-dimensional harmonic oscillator is addressed in **Appendix 3**.

3. Symmetry of the Hamiltonian and the Star Hamilton-Poisson Graphs

3.1. Star Hamilton-Poisson Graphs and the Noether Theorem

Now we address relations of the symmetry of the Hamiltonian to the emerging Hamilton-Poisson graph. Consider the hypothetic system described by the Hamiltonian $H(p_i, q_i)$ and five functions/obervables $f_1(p_i, q_i), \ldots, f_5(p_i, q_i)$. Assume that $\{H, f_1\} = 0$ and $\{H, f_2\} = 0$ is true. Thus, functions f_1 and f_2 are the symmetries of the Hamiltonian. We also assume $\{f_1, f_2\} = 0$, i.e. the symmetries of the Hamiltonian are commuting. It will be convenient now to represent the Hamilton-Poisson graph in the H-centered star form, as it is shown in **Figure 4**.

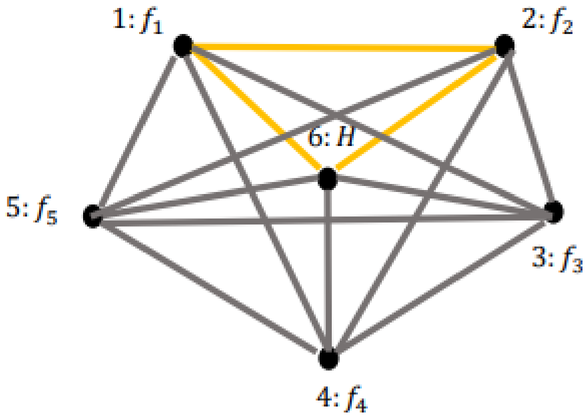

Figure 4. Star-like Hamilton-Poisson graph corresponding to the system described by Hamiltonian *H*. $\{H, f_1\} = 0$, $\{H, f_2\} = 0$ and $\{f_1, f_2\} = 0$ is assumed.

Every symmetry of the Hamiltonian corresponds to a vertex representing a conserved quantity, and the edge between *H* and this vertex is gold. Thus, gold edge $f \leftrightarrow H$ means: *f* is the symmetry of Hamiltonian. This is a direct graphical encoding of Noether's theorem. We also assume: $\{H, f_3\} \neq 0$; $\{H, f_4\} \neq 0$; $\{H, f_5\} \neq 0$; $\{f_3, f_4\} \neq 0$; $\{f_3, f_5\} \neq 0$; $\{f_4, f_5\} \neq 0$. These links/edges are grey. All these results are shown in the star-like Hamilton-Poisson graph, depicted in **Figure 4**.

The graph, presented in **Figure 4** is symmetrical. It is easily seen that permutations of the functions $f_1(p_i, q_i), \ldots, f_5(p_i, q_i)$ do not impact the symmetry of the graph. A symmetry of a graph is an automorphism. The automorphism permutes the observables in such a way that gold edges remain gold, and silver edges remain silver. The symmetry of the Hamilton–Poisson graph is a graphical shadow of the algebra of symmetries of the Hamiltonian system. Graph automorphisms correspond to transformations of phase-space observables preserving Poisson-bracket relations. These transformations are precisely the symmetry transformations of the physical Hamiltonian. Symmetric subgraphs correspond to invariant subalgebras (Abelian or non-Abelian). The star structure centered on *H* isolates and visualizes Noether symmetries. So, the symmetry recognized the graph is not accidental - it is the direct combinatorial imprint of the physical symmetry of the dynamical system.

H-centered star-like graphs emerging for the rotation of the rigid body and oscillations of the two-dimensional harmonic oscillator are supplied in **Appendices 2-3**.

3.2. Cyclic Coordinates Within the Ramsey Approach

Let us generalize the introduced approach and extend it to the systems possessing cyclic coordinates. Consider the system described by the Hamiltonian $H = H(q_1, q_2, p_1, p_2, p_3)$. Coordinate q_3 is the cyclic one; thus, $p_3 = const.$ We introduce the bi-colored complete graph, in which $H, q_1, q_2, p_1, p_2, p_3$ are the vertices and the color of the links/edges is defined by Eqs. 3-4. Consider Eqs. 12:

$$\{q_i, q_k\} = 0;\ \{p_i, p_k\} = 0;\ \{p_i, q_k\} = \delta_{ik}, i, k = 1, \ldots, 3. \tag{12}$$

Also, consider $\{H, p_3\} = 0$, due to $p_3 = const.$ This yields the graph depicted in **Figure 5**:

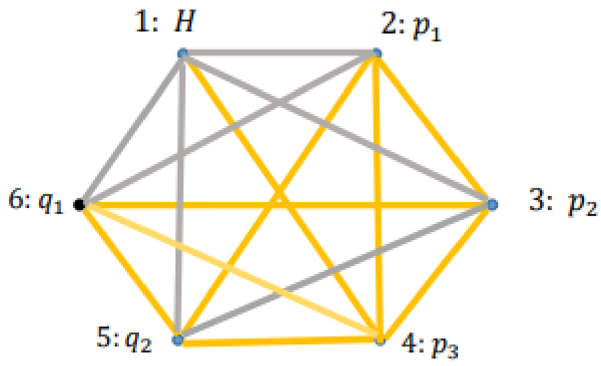

Figure 5. Complete, bi-colored, Hamilton-Poisson graph corresponding to the system described by the Hamiltonian $H = H(q_1, q_2, p_1, p_2, p_3)$. Coordinate q_3 is the cyclic one; $p_3 = const.$

The graph is easily re-shaped into the star-like form, shown in **Figure 6**. The graphs, depicted in **Figures 5-6** has nine gold and six silver links/edges, so we are close to the Mantel–Turán limit; i.e. $n > 9$ links of the same color guarantee appearance on the monochromatic triangle in the bi-colored, complete graph containing six vertices 9-12]. We are close but do not get Mantel–Turán limit [9–12]. Thus, appearance of mono-colored triangles is not guaranteed. However, these triangles are present in the graph.

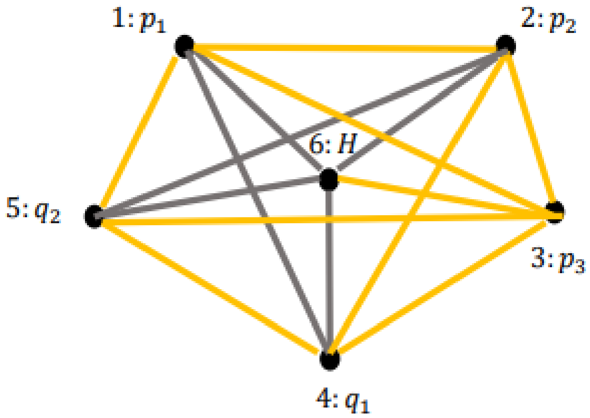

Figure 6. Star-like Poisson-Hamilton graph corresponding to the system described by the Hamiltonian $H = H(q_1, q_2, p_1, p_2, p_3)$. Coordinate q_3 is the cyclic one; $p_3 = const.$

Triangles $\{q_1, q_2, p_3\}$, $\{q_1, p_2, p_3\}$, $\{q_2, p_1, p_3\}$ and $\{p_1, p_2, p_3\}$ are monochromatic gold; triangles $\{p_2, q_2, H\}$ and $\{p_1, q_1, H\}$ are monochromatic silver. The meaning of this coloring is explained in detail in Section 2.1.

4. Analysis of the Systems Possessing the Infinite Degrees of Freedom

Consider the Hamiltonian systems whose phase space contains an infinite set of canonical pairs $\{(q_1, p_1), (q_2, p_2), \dots, (q_n, p_n), \dots\}$, i.e. countably infinite canonical degrees of freedom. As an example we can take a vibrating string of length L which Hamiltonian can be expanded into normal modes:

$$H(p_n, q_n) = \sum_{n=1}^{\infty} \left[\frac{p_n^2}{2} + \frac{\omega_n^2 q_n^2}{2}\right], \omega_n = \frac{\pi n c}{L}, \tag{13}$$

where c is the velocity of sound in the string. The canonical relations are $\{q_i, q_k\} = 0$; $\{p_i, p_k\} = 0$; $\{p_i, q_k\} = \delta_{ik}$. Consider infinite set of the functions/observables: $f_1(p_i, q_i), \dots . f_m(p_i, q_i), \dots$ The Poisson brackets are defined now as:

$$\{f_l, f_m\} = \sum_{i=1}^{\infty} \left(\frac{\partial f_l}{\partial q_i} \frac{\partial f_m}{\partial p_i} - \frac{\partial f_l}{\partial p_i} \frac{\partial f_m}{\partial q_i} \right), \tag{14}$$

under the condition that the series (14) converges. Now infinite set of the functions/observables: $f_1(p_i, q_i), \dots . f_m(p_i, q_i), \dots$ serve as the vertices of the infinite graph. Vertices are connected with the colored links. Colors of the links are prescribed with Eqs. (3-4). Thus, bi-colored, complete, infinite graph emerges. According to the infinite Ramsey theorem the complete graph K_X on the vertex set X, with edges colored gold and silver, contains an infinite monochromatic clique [23]. That is, there exists an infinite subset $Y \subset X$ such that all edges between points of Y have the same color (either all gold or all silver) [23]. Thus, infinite graph built on the infinite set of the functions/observables: $f_1(p_i, q_i), \dots . f_m(p_i, q_i)$ necessarily contains a monochromatic clique: either gold or silver. The suggested approach will work for Klein-Gordon and Yang-Mills fields. This result gives rise to the **Theorem 2**.

Theorem 2. Consider an infinite countable family of observables $\{(q_1, p_1), (q_2, p_2), \dots, (q_n, p_n), \dots\}$, for which the Poisson brackets $\{f_l, f_m\} = \sum_{i=1}^{\infty} \left(\frac{\partial f_l}{\partial q_i} \frac{\partial f_m}{\partial p_i} - \frac{\partial f_l}{\partial p_i} \frac{\partial f_m}{\partial q_i} \right)$ is well-defined, i.e. the series converges. Construct a graph whose vertices are the observables $f_1, f_2 \dots$ Vertices of the graph are connected with the gold link, when $\{f_l, f_m\} = 0$ takes place; they are connected with the silver link, when $\{f_l, f_m\} \neq 0$ is true. This yields a bi-colored complete infinite graph. Then, by the Infinite Ramsey Theorem, the complete graph on this countably infinite vertex set contains an infinite monochromatic clique.

5. Shannon Entropy of the Hamilton-Poisson Graphs

We recognize certain order in the Hamilton-Poisson graphs depicted in **Figures 2-6**. How this order may be quantified? It may be quantified with the Shannon entropy of the graph [24,25]. The Shannon entropy of the bi-colored Ramsey complete graph we denote S and it is introduced with Eq. 15:

$$S = -\sum_k P_k ln P_k, k \geq 3, \tag{15}$$

where P_k is the fraction of monochromatic k-polygons/polygons with k sides (whatever gold or silver-colored) in the given complete graph [25]. The sampling takes place over the entire set of monochromatic polygons, whatever their colors are. We exemplify this approach with the graph depicted in **Figure 6**. The distribution of polygons in the graph is supplied in **Table 1**.

Table 1. Distribution of convex, monochromatic polygons in the graph, depicted in **Figure 6**.

Color	Triangle	Quadrilaterals	Pentagons	Hexagon
Golden	4	5	4	0
Silver	2	0	0	0

The Shannon entropy of the graph S is calculated with Eq. 16:

$$S = -\left[\left(\frac{6}{15}\right) ln \left(\frac{6}{15}\right) + \left(\frac{5}{15}\right) ln \left(\frac{5}{15}\right) + \left(\frac{4}{15}\right) ln \left(\frac{4}{15}\right) \right] = 1.085. \tag{16}$$

The Shannon entropy S, supplied by Eq. 15, is adequately interpreted as the average uncertainty to find the monochromatic polygon (whatever is its color, gold or silver) within the set of monochromatic polygons appearing in the given. The value of the Shannon entropy is exhaustively defined by the distribution of polygons in the given complete, bi-colored graph, and it is independent of the exact shapes of the polygons [25].

The Shannon measure of the Hamilton-Poisson graph may be introduced in an alternative way with a pair of Shannon entropies: namely S_g and S_s. They are interpreted as follows: S_g is interpreted as an average uncertainty to find the monochromatic gold polygon in the given graph,

 doi:10.20944/preprints202512.0575.v1

S_s is, in turn, an average uncertainty to find the monochromatic silver polygon in the same graph [25]. In this case, sampling of polygons is carried out separately from the gold and silver colored subsets of convex polygons. Thus, a pair of Shannon entropies (S_a, S_b) corresponds to any Hamilton-Poisson graph. The pair of Shannon entropies is introduced with Eqs. 17-18:

$$S_g = -\sum_n P_{ng} lnP_{ng}\,, n \geq 3, \quad (17)$$

$$S_s = -\sum_i P_{is} lnP_{is},\ i \geq 3. \quad (18)$$

where P_{ng} is the fraction of monochromatic gold polygons with *n* gold, and P_{is} is the fraction of monochromatic convex silver polygons with *i b*-sides/silver edges in a given Hamilton-Poisson graph. Sampling of polygons is carried out separately from the gold and silver subsets of convex polygons [25]. We demonstrate this quantification with the Hamilton-Poisson graph depicted in **Figure 6**. For the graph shown in **Figure 6** the distribution of monochromatic polygons is supplied in **Table 1**. Thus, we calculate the pair (S_g, S_s) as follows:

$$S_g = -P_{3g}\ln P_{3g} - P_{4g}\ln P_{4g} - P_{5g}\ln P_{5g} = -\left(\frac{4}{13}\right) ln\left(\frac{4}{13}\right) - \left(\frac{5}{13}\right) ln\left(\frac{5}{13}\right) - \left(\frac{4}{13}\right) ln\left(\frac{4}{13}\right) = 1.092\ ,\ S_s = -P_{3s}\ln P_{3s} = -\left(\frac{2}{2}\right) ln\left(\frac{2}{2}\right) = 0. \quad (19)$$

Finally, we obtain the pair od Shannon entropies: $(S_g, S_s) = (1.092, 0)$.

6. Extension for the Hamiltonians Depending Explicitly on Time

The suggested approach is easily extended for the situation when Hamiltonian explicitly depends on time $H(p,q,t)$. A new coordinate $q_0 = t$ is introduced in the extended phase space. Its canonically conjugate momentum: $p_0 = -H(p,q,t)$. The Poisson brackets are now: $\{f_l, f_m\} = \sum_{i=0}^{n}\left(\frac{\partial f_l}{\partial q_i}\frac{\partial f_m}{\partial p_i} - \frac{\partial f_l}{\partial p_i}\frac{\partial f_m}{\partial q_i}\right)$, which include the term: $\frac{\partial f_l}{\partial t}\frac{\partial f_m}{\partial p_0} - \frac{\partial f_l}{\partial p_0}\frac{\partial f_m}{\partial t}$. Coloring of the links of the Poisson-Hamilton graph is defined by Eqs. 3-4. For any given time the graph containing six vertices will contain at least one monochromatic triangle $(R(3,3) = 6)$. Poisson-Hamilton graph for Caldirola–Kanai Hamiltonian explicitly depending on time is supplied in **Appendix 4** [26]. It is noteworthy that in spite of the fact that some of Poisson brackets calculated for the Caldirola–Kanai Hamiltonian depend explicitly on time, the coloring of the emerging graph does not evolve with time (see **Appendix 4**).

7. Discussion

Graph theory already opened new horizons in physics [27]. However, its Ramsey branch remains practically unexploited by physicists. The Ramsey-Hamiltonian construction developed in this work suggests that the algebraic structure of Hamiltonian dynamics possesses a universal combinatorial rigidity that has not been previously recognized. By representing Poisson-bracket relations between observables as edges of a bi-colored complete Ramsey graph, we obtain a combinatorial picture in which Hamiltonian systems cannot avoid forming monochromatic structures. These structures correspond to dynamically meaningful clusters: gold cliques represent mutually commuting (integrable) subsets of observables, while silver cliques represent irreducibly interacting subsets.

The crucial point is that the emergence of such clusters does not depend on the particular form of the Hamiltonian. No assumptions of symmetry, separability, integrability, or perturbative smallness are required. The phenomenon is guaranteed purely by the Ramsey theorem: every sufficiently large Hamilton–Poisson graph must contain a monochromatic triangle, and every infinite graph must contain an infinite monochromatic clique. This leads to the prediction of Combinatorially Enforced Dynamical Order (abbreviated CEDO), which asserts that any sufficiently large Hamiltonian system contains either integrable pockets or fully interacting pockets. In infinitedimensional systems this dichotomy becomes even sharper, yielding an emergent integrable sector or an emergent fully interacting sector.

These findings reveal a new structural layer in classical mechanics. Even systems that are conventionally regarded as non-integrable or chaotic must contain small, unavoidable islands of integrability; conversely, systems normally considered separable must also contain irreducible cores of interaction. Although the combinatorial result does not determine which type of cluster is realized, its inevitability implies that the fine structure of Hamiltonian dynamics possesses a universal combinatorial skeleton.

Let us fix the novelty of the introduced approach: traditional Hamiltonian mechanics can show that if a set of observables commute, then integrability follows. It also can show that if Poisson brackets are nonzero, observables are dynamically coupled, but cannot guarantee that any particular subset of observables must be mutually commuting or mutually interacting. Hamiltonian mechanics provides no existence theorem for such clusters. In other words: classical mechanics can analyze given integrable sets, but it cannot assert that integrable or fully interacting triplets must exist in every sufficiently large set of observables. The introduced Ramsey–Hamiltonian approach, however, proves that: in every Hamiltonian system with at least six observables, integrable or fully interacting dynamical pockets must appear unavoidably. This is a new type of physical inevitability.

The Hamilton–Poisson model predicts a new CEDO physical effect. which states that in any Hamiltonian system, regardless of its form or symmetry, any six observables necessarily contain either a completely integrable triple (mutually commuting; an Abelian subalgebra) or a completely interacting triple (mutually non-commuting). Classical Hamiltonian mechanics cannot produce such inevitability, since it lacks any existence theorems for mutually commuting or mutually interacting subsets. The Ramsey–Hamiltonian approach therefore reveals a physically meaningful and unavoidable structural pattern - mini-integrable islands or mini-interacting clusters - that must appear in every Hamiltonian system solely due to combinatorics, not dynamics.

The Ramsey–Hamiltonian perspective also hints at broader implications. Because Poisson brackets correspond to commutators in the quantum correspondence [28], similar combinatorial constraints should shape the operator algebra in quantum systems, influencing emergent symmetries, collective modes, or entanglement structures. Moreover, the framework may find applications in field theory, turbulence, plasma dynamics, geometric mechanics, or any setting where infinite families of canonical observables play a role.

Overall, the approach introduced here suggests that combinatorial theorems—traditionally distant from dynamical systems—may uncover universal hidden order in physical theories. The full implications of this structural viewpoint, particularly in quantum mechanics and field-theoretic contexts, remain open for future exploration.

The introduced coloring based on the Poisson brackets is not unique. The three-colored scheme may be suggested. In this scheme $\{f_l, f_m\} = 0$ corresponds to the gold link; $\{f_l, f_m\} = const \neq 0$ – violet link; $\{f_l, f_m\} = f(p,q) \neq const$ – corresponds to the silver link. It is established that $R(3,3,3) = 17$; in other words every complete three-colored graph containing 17 vertices/observables inevitably includes at least one monochromatic triangle, either gold, violet or silver.

Conclusions

We consider the very general physical systems described by the Hamiltonian $H(p_i, q_i, i = 1, \dots, N)$. We introduced a Ramsey–Hamiltonian framework, a new approach that embeds classical Hamiltonian mechanics into a combinatorial structure governed by Ramsey theory. The central idea is to represent a finite family of observables $H(p_i, q_i), f_1(p_i, q_i), \dots . f_j(p_i, q_i)$ as the vertices of a Hamilton–Poisson graph, in which each edge is colored according to the qualitative type of the corresponding Poisson bracket, namely: we color edges by $\{f_l, f_m\} = 0$ (color *A*) or $\{f_l, f_m\} = -\{f_m, f_l\} \neq 0$ (color *B*, $H(p_i, q_i)$ itself may be considered as one of observables). This embedding transforms the Hamiltonian mechanic into a discrete object/complete, bi-colored graph amenable to global, purely combinatorial theorems. A principal outcome of this translation is that Ramsey-theoretic inevitabilities acquire concrete physical meaning. For any two-coloring of the complete graph on six vertices, the classical Ramsey theorem guarantees the presence of a monochromatic triangle. In the Hamilton–Poisson interpretation, such triangles correspond to triplets of observables exhibiting uniform Poisson-bracket relations. A fully "gold" (zero-bracket) triangle identifies a mutually involutive triple — a structural signature of integrability or symmetry. A fully "silver" (non-zero-bracket) triangle indicates a triplet forming a non-abelian Poisson subalgebra, often hinting at the presence of rotational or Lie-type structures. When one vertex of the triangle is the Hamiltonian *H*, these monochromatic configurations distinguish, respectively, conserved quantities $\{H, f_i\} = 0$ from interacting dynamical generators $\{H, f_i\} \neq 0$.

The framework provides a novel bridge between dynamical symmetries and graph symmetries. Graph automorphisms of the Hamilton–Poisson diagram correspond to permutations of observables preserving Poisson relations; those that fix the Hamiltonian reflect genuine physical symmetries of the system. In this way, the structure of the graph directly encodes Noether-type information: invariants, symmetric subspaces, and algebraic structures emerge as combinatorial motifs.

A conceptual advantage of the Ramsey–Hamiltonian method is its non-perturbative (it does not rely on expansions in small parameters, linearization, or proximity to an integrable limit) and model-independent character. While traditional dynamical-systems analysis relies on differential properties, continuity arguments, or perturbation theory, Ramsey theory furnishes guarantees that hold for *every* possible coloring of sufficiently large sets of observables. Thus, certain algebraic substructures must exist regardless of the detailed form of the Hamiltonian. This yields global constraints on the possible organization of observables in any high-dimensional mechanical system.

The proposed viewpoint also suggests a path toward new invariants for classification. Where symplectic or spectral invariants describe continuous aspects of dynamics, Ramsey-graph invariants capture discrete structural information: monochromatic cliques, symmetry groups of the Hamilton-Poisson graph, and minimal subsets required for guaranteed algebraic configurations. These invariants are insensitive to canonical transformations of the Hamiltonian but sensitive to the combinatorial pattern of Poisson dependencies. It is also noteworthy that the coloring of the Hamilton-Poisson graph may appear as the integral of the motion.

Finally, the framework is naturally extensible. It invites exploration of higher-order Ramsey numbers to study larger algebraic structures, quantum analogues *via* commutator graphs, dynamical evolution of colorings under canonical flows, and computational methods for detecting physically meaningful motifs in large observable sets. Taken together, the Ramsey–Hamiltonian approach offers a new combinatorial lens on the architecture of Hamiltonian mechanics, enriching the classical picture with structural results that are both rigorous and universally valid.

Appendix 1

A.1 Analysis of 1D Systems

We start our analysis from a simple example of 1D harmonic oscillator. Thus, the Hamiltonian looks as follows:

$$H(p, x) = \frac{1}{2m}p^2 + \frac{1}{2}m\omega^2 x^2. \qquad \text{(A1.1)}$$

Now, let us exemplify our approach with two graphs built of three vertices, namely: $\{H, p, L\}$, where *L* is the angular momentum of the particle, and: $\{H, p, x\}$. Consider that the angular momentum *L* is zero for 1D harmonic oscillator. Hence, we calculate: $\{H, p\} = m\omega^2 x$; $\{H, L\} = 0$; $\{p, L\} = 0$, $\{H, x\} = -\frac{p}{m}$; $\{p, x\} = -1$; $\{x, L\} = 0$; $\{p, L\} = 0$; $\{x, L\} = 0$; we get $\{p, x\} = -1 = const$. The graphs built according to the introduced coloring procedure are depicted in **Figure A.1.1**. We recognize that the graph built of *H*, *L*, *p* vertices is bi-colored (**Figure A.1.1A**); whereas, the graph built of *H*, *p*, *x* vertices is mono-colored **(Figure A.1.1.B**).

Thus, we conclude that *x*, *p* and *H* form a fully interacting triple and could not be simultaneously conserved.

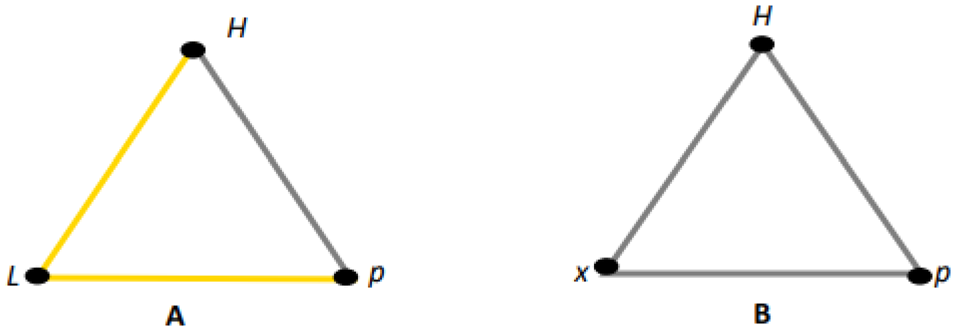

Figure A1.1. **A**. Bi-colored graph built for 1D harmonic oscillator. **A**. *H*, *L* and *p* are the vertices of the graph. **B**. *H*, *p*, and *x* are the vertices of the graph. Coloring of the edges of the graph is established by Eq. 3-4.

Now we exemplify our approach with the second instructive example, represented by a two-body (*M*, *m*) problem of the celestial mechanics (star-planet system), seen in the center-of-mass references in which:

$$H(p,r) = \frac{1}{2\mu}p^2 - \frac{GMm}{r}, \qquad \text{(A1.2)}$$

where μ is the effective mass, $\vec{p} = \mu\frac{d\vec{r}}{dt}$, *r* is the distance between the bodies, and *G* is the gravity constant; the angular momentum; $\vec{L} = \vec{r} \times \vec{p};\ L_i = \varepsilon_{ijk}r_jp_k$. The angular moment $\vec{L}$ is conserved, thus the motion of the effective mass μ occurs in the fixed plane. We calculate: $\{H,p\} = \frac{GMm}{r^2}$ $\{H,L\} = 0$ $\{p,L\} = 0;$ $\{H,r\} = -\frac{p}{\mu};$ $\{p,r\} = -1;$ $\{r,\ L\} = 0.$

It is easily seen that the harmonic oscillator and two-body star-planet problem are described by the same graphs. This may be understood, if consider that both systems are described by the general Hamiltonian:

$$H(p,x) = \frac{1}{2m}p^2 + V(x). \qquad \text{(A1.3)}$$

Within the silver-colored graph, of *H*, *p*, *x* built we have $\{x,H\} \neq 0$ and $\{x,H\} \neq 0$, Thus, we calculate from Eq. 6:

$$\{x,H\} = \frac{\partial H}{\partial p} = \frac{p}{m} = v = \dot{x} \neq 0, \qquad \text{(A1.4)}$$

$$\{p,H\} = -\frac{\partial H}{\partial x} = -\frac{\partial V}{\partial x} = \dot{p} \neq 0. \qquad \text{(A1.5)}$$

Thus, if $V(x) \neq 0$ and it means that the system evolves in time, the momentum changes (non-zero force), and the position changes (motion occurs). However, the coloring of the graph does not evolve with time and remain the same. And consequently, there is no equilibrium or static behavior in the system. We conclude that for the systems described by the potential $H = \frac{1}{2m}p^2 + V(x)$: i) coloring of the graphs built of three vertices H, p and x, established by Eqs. (3-4) is the same irrespectively to the specific kind of the potential $V(x)$; ii) coloring of the graph does not change with time and it is the integral of the motion; iii) coloring of the graph remains the same for centrally extended Galilean transformations, i.e. graphs are invariant relatively to Galilean transformations up to a central extension.

Again, we conclude that *r*, *p* and *H* form a fully interacting triple and could not be simultaneously conserved.

Preprints.org (www.preprints.org) | NOT PEER-REVIEWED | Posted: 5 December 2025 doi:10.20944/preprints202512.0575.v1

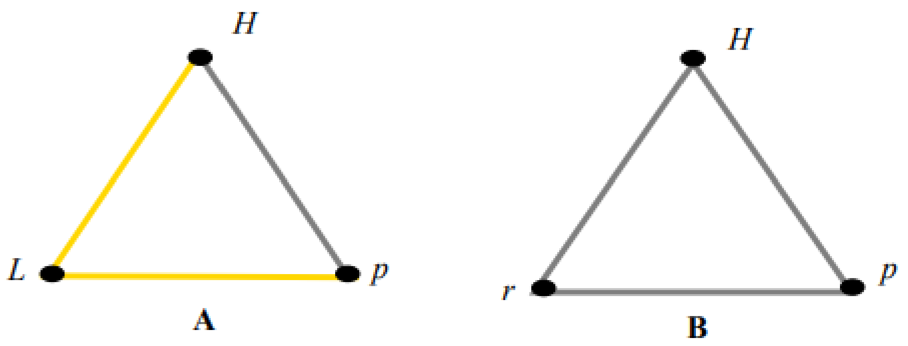

Figure A1.2. Bi-colored graphs built for two-body star-planet system. **A**. *H*, *L* and *p* are the vertices of the graph. **B**. *H*, *p*, and *r* are the vertices of the graph. Coloring of the edges of the graph is established by Eq. 3-4.

Appendix 2

A2. Analysis of the Rotation of Rigid Body

Now we consider the more complicated case of the rigid body rotating about the a single axis fixed relatively to the body (say axis *z*) . The Hamiltonian is given in this case by:

$$H = \frac{1}{2m}\left(p_x^2 + p_y^2 + p_z^2\right) + \frac{p_\theta^2}{2I} + V(x,y,z) = \frac{1}{2m}\left(p_x^2 + p_y^2 + p_z^2\right) + \frac{L_z^2}{2I} + V(x,y,z) \quad , \tag{A2.1}$$

where x, y, z is the position of the center of mass of the body, p_x, p_y, p_z linear momentum of the center of mass of the body, θ angle of rotation momentum about the body fixed axis (say *z*), $p_\theta = I\dot{\theta} = L_z$ – angular moment around fixed axis *z*. For a sake of clarity assume: $p_y = p_z = 0; V(x,y,z) = V(x), p_x = p;\ L_z = L.$

So the system is described by five parameters, namely: H, p, L, x, θ. Thus the Hamiltonian obtains the form:

$$H = \frac{p^2}{2m} + \frac{L^2}{2I} + V(x). \tag{A2.2}$$

We calculate the commutation relations:

$\{H, p\} = \frac{\partial V}{\partial x}$, $\{p, L\} = 0$, $\{H, L\} = 0$, $\{H, x\} = -\frac{p}{m}$, $\{p, x\} = -1$, $\{H, \theta\} = \frac{-L}{I}$, $\{l, \theta\} = -1$; $\{L, x\} = 0, \{p, L\} = 0,\ \{L, x\} = 0, \{x, \theta\} = 0.$

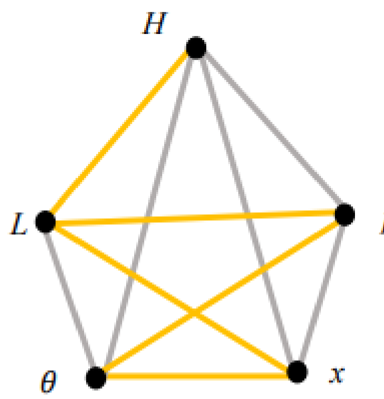

Figure A2.1. Bi-colored graph built for rigid body rotating about a single axis. *H*, *L*, *p*, *x*, *θ* are the vertices of the graph. Coloring of the edges of the graph is established by Eqs. 3-4.

The *H*-centered star-like graph corresponding to the graph, depicted in Figure A.2.1 is shown in **Figure A2.2**.

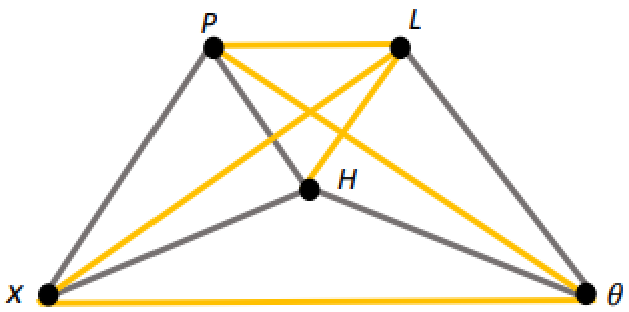

Figure A2.2. *H*-centered star-like graph corresponding to the Ramsey-Hamilton graph, depicted in **Figure A.2.1**.

There are no gold monochromatic triangles in the graph. Observables *H*, *P* and *x* form the silver monochromatic triangle and could not be simultaneously conserved.

Appendix 3

A3. Analysis of the Hamilton-Poisson Graph Obtained for the Two-Dimensional Harmonic Oscillator

We consider the two-dimensional isotropic harmonic oscillator. The Hamiltonian of the system is defined in the canonical phase space (x, y, p_x, p_y) as:

$$f_1 = H = \frac{1}{2}m\left(p_x^2 + p_y^2\right) + \frac{1}{2}m\omega^2(x^2 + y^2). \qquad \text{(A3.1)}$$

We construct a set of six functions $\{H, f_2, \dots, f_6\}$, playing the role of vertices in a complete graph. Edges are colored. Coloring is based on their Poisson bracket relationships (Eqs.3-4): $f_2 = x^2 + y^2$; $f_3 = xp_x + yp_y$; $f_4 = xp_y - yp_x$ (which is angular momentum); $f_5 = p_x^2 + p_y^2$; $f_6 = \left(xp_y - yp_x\right)^2$. The vertices of the graph are connected with a gold edge if the Poisson bracket between two functions vanishes: $\{f_l, f_m\} = 0$. Otherwise, they are connected with a silver edge when $\{f_l, f_m\} \neq 0$. The emerging graph is shown in **Figure A3.1**.

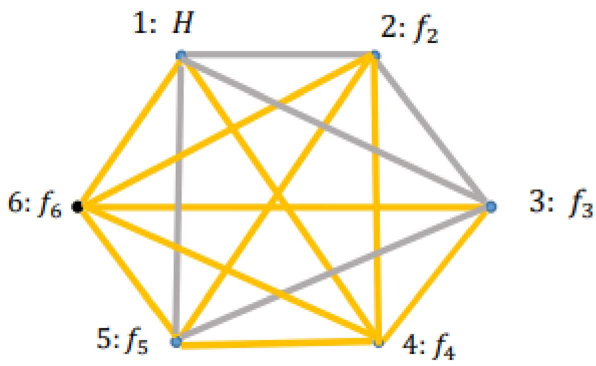

Figure A3.1. Bi-colored graph built for 2-d harmonic oscillator. $f_1 = H, f_2, f_3, f_4, f_5, f_6$ are the vertices of the graph. Coloring of the edges of the graph is established by Eqs. 3-4.

Now silver monochromatic triangles are: $\{H, f_2, f_3\}$ and $\{H, f_3, f_5\}$. These observables could not be simultaneously conserved. Gold monochromatic triangles are: $\{H, f_4, f_6\}, \{f_2, f_4, f_5\}$, $\{f_2, f_4, f_6\}, \{f_2, f_5, f_6\}$, $\{f_3, f_4, f_6\}$ and $\{f_4, f_5, f_6\}$. These are mutually involutive triads.

The *H*-centered graph, corresponding to the graph depicted in **Figure A.3.1** is shown in **Figure A3.2**.

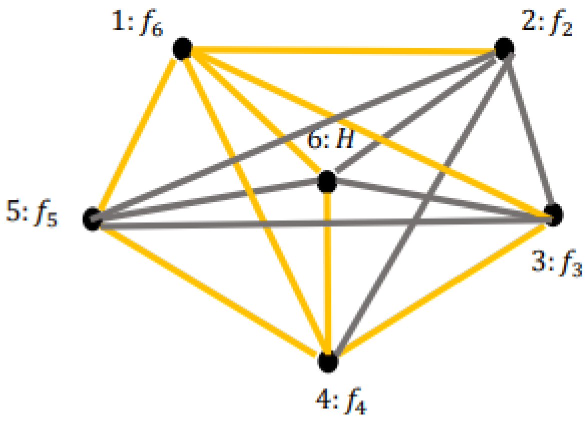

Figure A3.2. *H*-centered graph built for the 2-d harmonic oscillator corresponding to the graph depicted in **Figure A.3.1**.

Appendix 4

Poisson-Hamilton Graph for the Caldirola–Kanai Hamiltonian Explicitly Depending on Time

Consider the system described by the Caldirola–Kanai Hamiltonian, describing the motion of dissipating harmonic oscillator. We work now in the extended phase space, i.e. $q_0 = t$; $H = -p_0$ (see Section 6).

$$H(p,x,t) = \frac{1}{2me^{2\gamma t}}p^2 + \frac{1}{2}m\omega^2 e^{2\gamma t}x^2. \quad \text{(A4.1)}$$

The Poisson brackets are calculated as follows: $\{H,p\} = m\omega^2 e^{2\gamma t}x$, $\{H,x\} = -\frac{p}{me^{2\gamma t}}$; $\{p,x\} = -1$, $\{H,t\} = 1$ $\{p,t\} = 0$, $\{t,x\} = 0$. The corresponding Poisson-Hamilton graph is supplied in **Figure A.4.1**.

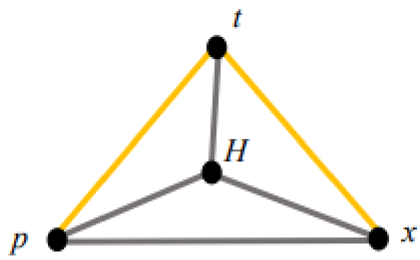

Figure A4.1. *H*-centered bi-colored complete graph emerging for the explicitly time-dependent Caldirola–Kanai Hamiltonian $H(p,x,t) = \frac{1}{2me^{2\gamma t}}p^2 + \frac{1}{2}m\omega^2 e^{2\gamma t}x^2$. .

In spite of the fact that some of the Poisson brackets calculated for the Caldirola–Kanai Hamiltonian depend explicitly on time, the coloring of the emerging graph, shown in **Figure A4.1**, does not evolve with time.

Acknowledgements: The author is indebted to Dr. Nir Shvalb for useful discussions.

Data availability statement: All data that support the findings of this study are included within the article.

Disclosure statement: The authors did not report any possible conflict of interest.

References

1. Landau LD, Lifshitz EM 1976 *Mechanics* Vol. 1 (3rd ed.) (Butterworth-Heinemann) Oxford, UK.

 doi:10.20944/preprints202512.0575.v1

2. Landau LD, Lifshitz EM 1975 *The Classical Theory of Fields* Vol. 2 (4th ed.), (Butterworth-Heinemann) Oxford.
3. Lanczos C 1970 *The Variational Principles of Mechanics* (Dover Publications) NY, USA.
4. Torres del Castillo GF 2018 *An Introduction to Hamiltonian Mechanics* Birkhauser, Cham, New York, USA.
5. Sardanashvily GA 1995 *Generalized Hamiltonian formalism for field theory: constraint systems* World Scientific, Singapore.
6. Giachetta G, Mangiarotti L, Sardanashvily G 2010, *Geometric Formulation of Classical and Quantum Mechanics* World scientific, Singapore.
7. Azuaje R, Escobar-Ruiz AM 2023 Canonical and canonoid transformations for Hamiltonian systems on (co)symplectic and (co)contact manifolds *J. Math. Phys*. **64**, 033501.
8. Ramsey FP 2009, On a Problem of Formal Logic. In *Classic Papers in Combinatorics*; Gessel, I., Rota, G.C., Eds.; Modern Birkhäuser Classics; Birkhäuser: Boston, MA, USA, pp. 264–286.
9. Graham RL, Rothschild BL, Spencer JH 1990 *Ramsey Theory*, 2nd ed.; Wiley-Interscience Series in Discrete Mathematics and Optimization; John Wiley & Sons, Inc.: New York, NY, USA, pp. 10–110.
10. Di Nasso M, Goldbring I, Lupini M 2019, *Nonstandard Methods in Combinatorial Number Theory* Lecture Notes in Mathematics; Springer: Berlin/Heidelberg, Germany, Vol. 2239.
11. Katz M, Reimann J 2018 *An Introduction to Ramsey Theory: Fast Functions, Infinity, and Metamathematics* Student Mathematical Library (American Mathematical Society) Providence, RI, USA, Volume 87, pp. 1–34.
12. Graham R, Butler S 2015 *Rudiments of Ramsey Theory* 2nd ed. (American Mathematical Society) Providence, RI, USA, pp. 7–46.
13. Li Y, Lin Q 2020 *Elementary Methods of the Graph Theory* Applied Mathematical Sciences, (Springer) Cham, Switzerland, pp. 3–44.
14. Chartrand G, Chatterjee P, Zhang P Ramsey chains in graphs 2023, *Electron. J. Math*. **6**, 1–14.
15. [15] de Gois C, Hansenne K, Gühne O 2023, Uncertainty relations from graph theory *Phys. Rev. A*, **107**, 062211 .
16. Xu Z-P, Schwonnek R, Winter A 2024, Bounding the Joint Numerical Range of Pauli Strings by Graph Parameters *PRX Quantum*, **5**, 020318.
17. Hansenne K, Qu R, Weinbrenner LT, de Gois C, Wang H, Ming Y, Yang Z, Horodecki P, Gao W, Gühne O Optimal overlapping tomography, arXiv: 2408.05730, 2024.
18. Wouters J, Giotis A, Kang R, Schuricht D, Fritz L 2022, Lower bounds for Ramsey numbers as a statistical physics problem *J. Stat. Mech*. **2022**, 0332.
19. Bormashenko Ed 2025, Variational principles of physics and the infinite Ramsey theory *Phys. Scr*. **100**, 01504.
20. Bormashenko Ed, Shvalb NA 2024, Ramsey-Theory-Based Approach to the Dynamics of Systems of Material Points *Dynamics* **4** (4), 845-854.
21. Frenkel M, Shoval Sh Bormashenko Ed 2023 Fermat Principle, Ramsey Theory and Metamaterials *Materials* **6** (24) 7571.
22. Choudum SA, Ponnusamy B 1999 Ramsey numbers for transitive tournaments *Discrete Mathematics* **206**, 119–129.
23. Soifer A 2009 *From Pigeonhole Principle to Ramsey Principle*. In: The Mathematical Coloring Book. Springer, New York, NY, pp. 263-265.
24. Shannon CE 1948 A Mathematical Theory of Communication. *Bell Syst. Tech. J.* **27**, 379–423.
25. Frenkel N, Shoval Sh 2023 Bormashenko Ed. Shannon Entropy of Ramsey Graphs with up to Six Vertices *Entropy*, **25** (10), 1427.
26. Dodonov VV, Man'ko VI 1979, Coherent states and the resonance of a quantum damped oscillator, *Phys. Rev. A* **20**, 550.
27. Kottos T, Smilansky U 1997, Quantum Chaos on Graphs *Phys. Rev. Lett*. **79** (24), 4794-4797.
28. Landau LD, Lifshitz EM 1991 *Quantum mechanics: non-relativistic theory* Volume 3 of Course of Theoretical Physics, 3rd Ed., (Pergamon Press) Oxford, UK.

doi:10.20944/preprints202512.0575.v1